Bond between FRP composites and concrete: Assessment of design procedures and analytical models

Tommaso D'Antino, Carlo Pellegrino *

University of Padova, Department of Civil, Environmental and Architectural Engineering, Via Marzolo 9, 35131 Padova, Italy

Received 24 August 2013
Received in revised form 21 December 2013
Accepted 26 December 2013
Available online 4 January 2014

1. Introduction

In the last few decades, the civil engineering community and construction industry have witnessed a rapid growth of interest about the fibre-reinforced composites. Great attention has been devoted particularly to fibre reinforced polymer (FRP) composites, comprised of high strength fibres embedded within a thermosetting organic matrix, usually epoxy resin. Rehabilitation and strengthening of reinforced concrete (RC) structures with externally bonded (EB) FRP composites represent a sustainable alternative to new construction because they allow for an extension of the original service life and therefore prevent demolition of existing structures. The necessity of strengthening RC structures may depend on different reasons, such as ageing, improper design or construction, change of the design loads, lack of maintenance, damage caused by environmental factors or seismic events.

The use of externally bonded FRP composites has shown to be an effective technique for rehabilitation/strengthening/retrofitting of RC structures in shear (see for instance some works developed at the University of Padova as [2–4]), flexural [5,6], and confinement [7,8] applications. Although many experimental and analytical works are available in literature, some issues concerning this technique are still under discussion. One of the most important issues is represented by proper design against various debonding failure modes [9–14], including cover separation, plate end interfacial debonding, intermediate flexural crack-induced interfacial debonding, and diagonal crack-induced interfacial debonding. Several analytical models for the evaluation of the FRP–concrete bond strength were proposed by various authors and some of them are included in design codes/recommendations/guidelines.

This work presents an assessment of twenty analytical models for the evaluation of the bond strength between FRP and concrete. The assessment was carried out by means of a wide database including several experimental results available in literature.

Some authors [15] showed that there exist many experimental setups to evaluate the FRP–concrete bond strength. Nevertheless a shared standard test procedure does not exist yet. The most diffused experimental setups are represented by the single shear test, the double shear test and the bending test (Fig. 1). In the former the FRP composite is bonded to one face of a concrete prism and the fibres are usually pulled while the prism is restrained. Double

* Corresponding author. Tel./fax: +39 0498275618.
E-mail address: carlo.pellegrino@unipd.it (C. Pellegrino).

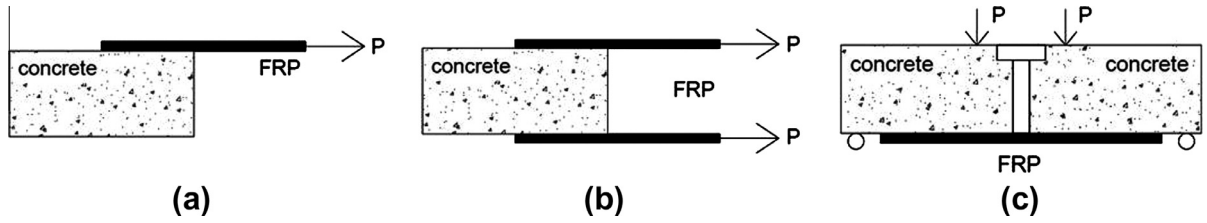

Fig. 1. Test setups for the evaluation of the FRP–concrete bond strength; (a) single shear test, (b) double shear test, and (c) small-scale bending test.

shear test consists in pulling two concrete prisms connected one to the other by means of FRP composites bonded on opposite faces. In bending tests the FRP composite is bonded to the bottom of a beam subjected to flexure. Bending tests are sometimes carried out on small scale specimens where a notch or a hinge is provided in order to initiate debonding at a specific cross-section. However, the combination of results related to both small- and full-scale specimens is arguable due to different mechanisms and resisting contributions developing in small- and full-scale beams. For this reason, in this work the experimental tests of small-scale notched beams were discarded and only the results of full-scale strengthened RC beams subjected to bending tests were included in the database.

It was observed that the various test setups could lead to different results for the same amount and type of FRP [15]. For this reason, the assessment was carried out distinguishing between the various test setups to give some elements for defining a shared test setup allowing to properly measure the bond strength in FRP–concrete joints. Further, the influence of the FRP composite preparation, e.g. post-impregnated sheets or pre-impregnated laminates, was investigated.

Since in the literature there is little information about the accuracy of the analytical models regarding the effective bond length, i.e. the minimum length needed to fully develop the bond strength capacity, a comparison between experimental and analytical provisions of the effective bond length is shown and commented as well.

2. Current analytical models for predicting FRP–concrete bond strength

Twenty analytical bond strength models were collected from the literature. The main equations of the codes/recommendations/guidelines included in this work are briefly recalled for the sake of clarity. The same notation adopted by the authors is reported here. In each of the following models the elastic modulus, thickness and width of the FRP composite are indicated as E_f, t_f, and b_f, respectively. Further details about the analytical formulations can be found in the original documents.

fib Bulletin 14-T.G. 9.3 [16]

The maximum force $N_{fa,\max}$ which can be anchored by the FRP can be obtained as:

$$N_{fa,\max} = \alpha c_1 k_c k_b b \sqrt{E_f t_f f_{ctm}} \tag{1}$$

where α is a reduction factor taking into account the influence of inclined cracks; f_{ctm} is the mean value of the concrete tensile strength; c_1 may be obtained through calibration with test results and, in case of CFRP, is equal to 0.64; k_c is a factor accounting for the state of compaction of the concrete, and k_b is a geometrical coefficient:

$$k_b = 1.06\sqrt{\frac{2 - b_f/b}{1 + b_f/400}} \geq 1 \tag{2}$$

where b is the cross-section width of the strengthened element. If the bonded length l_b is less than the effective bond length $l_{b,\max}$, the maximum force $N_{fa,\max}$ is reduced according to:

$$N_{fa} = N_{fa,\max}\frac{l_b}{l_{b,\max}}\left(2 - \frac{l_b}{l_{b,\max}}\right) \tag{3}$$

CNR DT-200 [1]

The Italian document CNR DT-200 [1] proposes a formulation similar to that of the *fib* Bulletin 14-T.G. 9.3 [16]. Using a fracture mechanics approach it quantifies the maximum stress in the FRP composite, f_{fdd}, as a function of the fracture energy, Γ_{Fk}, of the FRP–concrete interface. The maximum stress which can be carried by the FRP–concrete joint is obtained as:

$$f_{fdd} = \frac{k_{cr}}{\gamma_{f,d}\sqrt{\gamma_c}}\sqrt{\frac{2E_f\Gamma_{Fk}}{t_f}} \tag{4}$$

where $\gamma_{f,d}$ and γ_c are the composite and concrete safety factors, respectively.

If the bonded length l_b is less than the effective bond length l_e, the maximum stress is reduced according to Eq. (5):

$$f_{fdd,rid} = f_{fdd}\frac{l_b}{l_e}\left(2 - \frac{l_b}{l_e}\right) \tag{5}$$

The maximum force which can be anchored by the FRP is finally calculated multiplying the cross-sectional area of the composite by the maximum stress obtained with Eqs. (4) and (5). The reduction factor k_{cr} distinguishes between different kinds of delamination (k_{cr} = 1 in case of end delamination, k_{cr} = 3 in case of intermediate delamination due to flexural cracking).

The fracture energy of the FRP–concrete interface is calculated as:

$$\Gamma_{Fk} = 0.03\ k_b\sqrt{f_{ck}f_{ctm}} \tag{6}$$

where f_{ck} is the characteristic compressive cylinder strength of concrete and k_b is a geometrical factor equal to:

$$k_b = 1.06\sqrt{\frac{2 - b_f/b}{1 + b_f/400}} \geq 1 \tag{7}$$

A new version of the Italian recommendations CNR DT-200 is now under preparation but not officially published. It provides some modifications of the existing formulations according to the most recent experimental studies trying to improve the accuracy of the analytical provisions.

ACI 440.2r [17]

The Guide of the American Concrete Institute calculates the maximum bond strength, in case of flexural strengthening, multiplying the maximum strain in the FRP composite at the ultimate limit state, named effective strain ε_{fe}, by the elasticity modulus of the FRP composite E_f, assuming perfectly elastic behaviour. The effective strain ε_{fe} in the FRP composite is limited to the strain value at which debonding may occur, ε_{fd}, as defined in Eqs. (8) and (9). The effective stress in the FRP reinforcement f_{fe} is then obtained considering the mode of failure for a given neutral axis depth, as shown in Eqs. (9) and (10). If the left term of the inequality (Eq. (9)) controls, the member fails due to concrete crushing; if

the right term of the inequality controls the member fails due to FRP failure:

$$\varepsilon_{fd} = 0.41\sqrt{\frac{f'_c}{nE_f t_f}} \leqslant 0.9\varepsilon_{fu} \tag{8}$$

$$\varepsilon_{fe} = \varepsilon_{cu}\left(\frac{d_f - c}{c}\right) \leqslant \varepsilon_{fd} \tag{9}$$

$$f_{fe} = E_f \varepsilon_{fe} \tag{10}$$

where, in this guide, n indicates the number of plies of FRP reinforcement and t_f is the thickness of one ply of FRP reinforcement, f'_c is the specified concrete compressive strength, ε_{cu} is the ultimate axial strain of unconfined concrete, taken as 0.003; d_f and c are the FRP composite depth and neutral axis depth, respectively. The maximum force which can be anchored by the composite is finally obtained multiplying the area of the composite by the effective stress f_{fe}.

In case of shear or simply axial strengthening the maximum bond strength is calculated multiplying the maximum strain in the FRP reinforcement at the ultimate limit state, ε_{fe}, according to Eq. (11) (valid in case of U-wraps or bonded face plies), by the FRP elasticity modulus, assuming perfectly elastic behaviour as for flexural strengthening (Eq. (10)). In this case the effective strain is limited by means of an empirical coefficient, k_v as follows:

$$\varepsilon_{fe} = k_v\ \varepsilon_{fu} \leqslant 0.004 \tag{11}$$

$$k_v = \frac{k_1 k_2 l_e}{11{,}900\varepsilon_{fu}} \leqslant 0.75 \tag{12}$$

k_1 and k_2 are modification factors taken equals to 1.0 in case of pure axial tension.

In addition to these models, sixteen other formulations proposed by various authors were considered for the assessment. The expressions for computing the maximum force N_f carried by the FRP–concrete joint are here reported for the sake of completeness. The meaning of symbols is indicated in the following if not specified above.

CNR DT-200 R1 [18]

A new version of the Italian guidelines, CNR DT-200 R1 [18] has been recently published. It provides new equations with the aim of improving the accuracy of the previous version [1]. New equations for computing the fracture energy, the effective bond length, and the FRP–concrete strength are provided. The maximum stress f_{fdd} that can be carried by the composite preventing the plate end debonding failure is calculated as:

$$f_{fdd} = \frac{k_{cr}}{\gamma_{f,d}}\sqrt{\frac{2E_f \Gamma_{Fd}}{t_f}} \tag{13}$$

$$f_{fdd,rid} = f_{fdd}\frac{l_b}{l_e}\left(2 - \frac{l_b}{l_e}\right) \quad \text{for } l_b < l_e \tag{14}$$

The specific fracture energy Γ_{Fd} is computed according to Eq. (15):

$$\Gamma_{Fd} = \frac{k_b \cdot k_G}{FC} \cdot \sqrt{f_{cm} \cdot f_{ctm}} \tag{15}$$

$$k_b = \sqrt{\frac{2 - b_f/b}{1 + b_f/b}} \geq 1 \tag{16}$$

where $k_G = 0.023$ in case of pre-impregnated laminate, and $k_G = 0.037$ in case of post-impregnated sheet. FC is an additional safety factor. In order to avoid the intermediate crack-induced debonding failure the maximum FRP stress must be less or equal to $f_{fdd,2}$:

$$f_{fdd,2} = \frac{k_q}{\gamma_{f,d}}\sqrt{\frac{E_f}{t_f} \cdot \frac{2 \cdot k_b \cdot k_{G,2}}{FC} \cdot \sqrt{f_{cm} \cdot f_{ctm}}} \tag{17}$$

where $k_{G,2}$ is an empirical coefficient equal to 0.10, and $k_q = 1.25$ in case of distributed load, and $k_q = 1.0$ in all other cases.

Van Gemert [19]:

$$N_f = 0.5 \cdot b_f \cdot l_b \cdot f_{ctm} \tag{18}$$

Tanaka [11]:

$$N_f = (6.13 - \ln l_b) \cdot b_f \cdot l_b \tag{19}$$

Hiroyuki and Wu [20]:

$$N_f = b_f \cdot l_b (5.88 \cdot l_b^{-0.669}) \cdot \tag{20}$$

where the quantity within the brackets represents the average bond strength τ_u expressed in MPa, and l_b within the brackets is expressed in centimetres.

Maeda et al. [11]:

$$N_f = 110.2 \times 10^{-6} \cdot E_f \cdot t_f \cdot b_f \cdot l_e \tag{21}$$

Neubauer and Rostàsy [21]:

$$N_f = 0.64 \cdot k_p \cdot b_f \cdot \sqrt{f_{ctm} \cdot E_f \cdot t_f} \quad \text{if } l_b \geqslant l_e \tag{22}$$

$$N_f = 0.64 \cdot k_p \cdot b_f \cdot \sqrt{f_{ctm} \cdot E_f \cdot t_f} \cdot \frac{l_b}{l_e} \cdot \left(2 - \frac{l_b}{l_e}\right) \quad \text{if } l_b < l_e \tag{23}$$

where k_p is a geometrical factor equal to:

$$k_p = \sqrt{1.125\frac{2 - b_p/b_c}{1 + b_p/400}} \tag{24}$$

Khalifa et al. [22]:

$$N_f = 110.2 \times 10^{-6} \cdot \left(\frac{f_{ck}}{42}\right)^{2/3} E_f \cdot t_f \cdot b_f \cdot l_e \tag{25}$$

Adhikary and Mutsuyoshi [23]:

$$N_f = b_f \cdot l_b \cdot (0.25 \cdot f_{ck}^{2/3}) \tag{26}$$

Chen and Teng [11]:

$$N_f = 0.315 \cdot \beta_p \cdot \beta_L \cdot \sqrt{f_{ck}} \cdot b_f \cdot l_e \tag{27}$$

$$\beta_p = \sqrt{\frac{2 - b_f/b}{1 + b_f/b}} \tag{28}$$

$$\beta_l = \begin{cases} 1 & \text{if } l_b \geq l_e \\ \sin\frac{\pi l_b}{2 l_e} & \text{if } l_b < l_e \end{cases} \tag{29}$$

De Lorenzis et al. [24]:

$$N_f = b_f \cdot \sqrt{2 \cdot E_f \cdot t_f \cdot G_f} \tag{30}$$

where G_f is the fracture energy per unit area of the joint, assumed equal to 1.43 Nmm/mm^2. It should be noted that Eq. (30) was originally proposed by Taljsten [9].

Yang et al. [13]:

$$N_f = \left(0.5 + 0.08 \cdot \sqrt{\frac{E_f \cdot t_f}{1000}}\right) \cdot b_f \cdot l_e \cdot 0.5 \cdot f_{ctm} \tag{31}$$

Izumo [25]:

$$N_f = (3.8 \cdot f_{ck}^{2/3} + 15.2) \cdot l_b \cdot b_f \cdot E_f \cdot t_f \times 10^{-3} \tag{32}$$

Iso [25]:

$$N_f = b_f \cdot l_e \cdot 0.93 \cdot f_{ck}^{0.44} \tag{33}$$

Sato [25]:

$$N_f = (b_f + 7.4) \cdot l_e \cdot 2.68 \cdot f_{ck}^{0.2} \cdot E_f \cdot t_f \times 10^{-5} \tag{34}$$

Dai et al. [26]:

$$N_f = (b_f + 7.4) \cdot \sqrt{2 \cdot E_f \cdot t_f \cdot G_f} \tag{35}$$

$$G_f = 0.514 f_c^{0.236} \tag{36}$$

where f_c is the compressive strength of concrete.

Lu et al. [13]:

$$N_f = \beta_l \cdot b_f \cdot \sqrt{2 \cdot E_f \cdot t_f \cdot G_f} \tag{37}$$

$$G_f = 0.308 \beta_w^2 \sqrt{f_t} \tag{38}$$

$$\beta_w = \sqrt{\frac{2.25 - b_f/b}{1.25 + b_f/b}} \tag{39}$$

where f_t is the concrete tensile strength and $\beta_l = \sin[(\pi \cdot l_b)/(2 \cdot l_e)]$ is the effective bond length factor.

Camli and Binici [27]:

$$N_f = \sqrt{\tau_f \cdot \delta_f} \cdot \sqrt{E_f \cdot t_f} \cdot b_f \cdot \tanh\left(\frac{\theta \cdot l_b}{l_e}\right) \tag{40}$$

$$\theta = \sqrt{\frac{\tau_f}{\delta_u \sqrt{f_c}}} \tag{41}$$

$$\tau_f = 3.5 f_c^{0.19} \tag{42}$$

$$\delta_u = f_c^{\alpha} \left(\frac{l_b}{l_e}\right)^{\beta} \left(\frac{b_f}{b}\right)^{\gamma} \tag{43}$$

where α, β, and γ are coefficient found through non-linear regression analysis and equal to −0.4, 0.80, and 0.40, respectively.

The above analytical models were applied without using partial safety factors, assuming that they provide the mean value of the maximum force which can be carried by the FRP–concrete joint.

3. Experimental database

A wide experimental database was collected from the literature and used to assess the analytical models for the FRP–concrete bond strength described above. The database contains 404 specimens, 231 of which tested using the single shear test setup [10,11,13,28–34], including both laminates (25 specimens) and sheets (206 specimens); 60 specimens strengthened with sheets tested using the double shear test setup [11,13,14]; 124 specimens tested in bending [35–40,42], including both laminates (74 specimens) and sheets (39 specimens). The detailed characteristics of the specimens included in the database are reported in Appendix A.

4. Assessment of the FRP–concrete bond strength models

The accuracy of each analytical model was evaluated comparing the experimental bond strength results with the corresponding analytical predictions. The results are provided in terms of maximum experimental (measured) force $P_{\exp,i}$, and theoretical force $P_{th,i}$, that can be carried by the FRP–concrete interface of the ith specimen. Experimental vs. theoretical bond strength diagrams were built [13,38,41]. The accuracy of the various models was assessed through computing the coefficient of variation *CoV*, defined by Eq. (47). $CoV = 0$ indicates perfect matching between experimental and analytical bond strength. In addition, the average *Avg*, and the standard deviation *StD* were calculated according to Eqs. (45) and (46), respectively:

$$x_i = P_{\exp,i}/P_{th,i} \tag{44}$$

$$Avg = \frac{\sum_{i=1}^{n} x_i}{n} \tag{45}$$

$$StD = \sqrt{\frac{\sum_{i=1}^{n} (x_i - Avg)^2}{n}} \tag{46}$$

$$CoV = \sqrt{\frac{\sum_{i=1}^{n} (x_i - Avg_{ref})^2}{n}} \tag{47}$$

Fig. 2 shows, as an example, the diagrams for CNR DT-200 [1], *fib* Bulletin 14 T.G. 9.3 [16], ACI 440.2R [17], and CNR DT-200 R1 [18]. The values above the line $P_{\exp}/P_{th} = 1$ are conservative since the experimental bond strength is greater than the corresponding analytical prediction, whereas values below the line $P_{\exp}/P_{th} = 1$ are unconservative.

The statistical procedure was carried out distinguishing between different test setups, i.e. single shear test (*Single*), double shear test (*Double*), and bending test (*Bending*). The statistical analysis was also developed distinguishing between FRP post-impregnated sheets (*Sheet*) and FRP pre-impregnated laminates (*Laminate*). Table 1 summarises the results for all considered models, listing the coefficient of variation *CoV* together with the corresponding average value of the ratio between the experimental and theoretical value *Avg*.

Analysing the results obtained for the most important guidelines (CNR DT-200 [1], *fib* Bulletin 14 T.G. 9.3 [16], and ACI 440.2R [17], CNR DT-200 R1 [18]), it can be noted that the predictions are sometimes non-conservative (Fig. 2). The ACI 440.2R [17] provides more conservative predictions in terms of maximum FRP–concrete bond strength with respect to the other models, but its accuracy, measured in terms of coefficient of variation, is rather poor. This can be due to the fact that the American formulations are based on the analysis of few experimental data.

The results reported in Table 1 shows that some models are more accurate when compared to double shear tests whereas others are more accurate when compared to single shear tests. The best result in terms of coefficient of variation was obtained by the model of Lu et al. [13] for single shear tests ($CoV = 0.18$), whereas the model of Neubauer and Rostàsy [21] gives the best result for double shear tests ($CoV = 0.22$). It should be noted that, except for CNR DT-200 [1] ($CoV = 0.33$), the analytical calculations are particularly inaccurate for full-scale bending tests. Furthermore, it seems that the accuracy of the Italian Guidelines reduces from the previous to the new version for bending tests and when laminates are used.

The general reduction of accuracy when analytical models are compared with results related to bending tests can be justified by the fact that most of the analytical models were formulated and calibrated mostly using single and double shear tests, because of their lower cost with respect to full-scale bending tests. It should be noted that, in the case of full-scale bending tests, the maximum load that can be carried by the FRP–concrete interface is not directly measured but it is calculated according to the flexural moment and the corresponding measured beam failure load ($2P$ in Fig. 1c). Therefore, the hypotheses on which the above calculations are based, mainly related to the assumption that the cross-sections of the beam remain plane, have to be taken into account for the interpretation of the results of this study.

A clear influence of the material preparation (e.g. between post-impregnated sheet and pre-impregnated laminate composites) was not observed, but it has to be pointed out that laminate composites are usually employed in case of full-scale bending test, whereas sheets composites are more diffused in case of single and double shear test. Furthermore, double shear tests carried out using FRP laminates were not available at the time in which

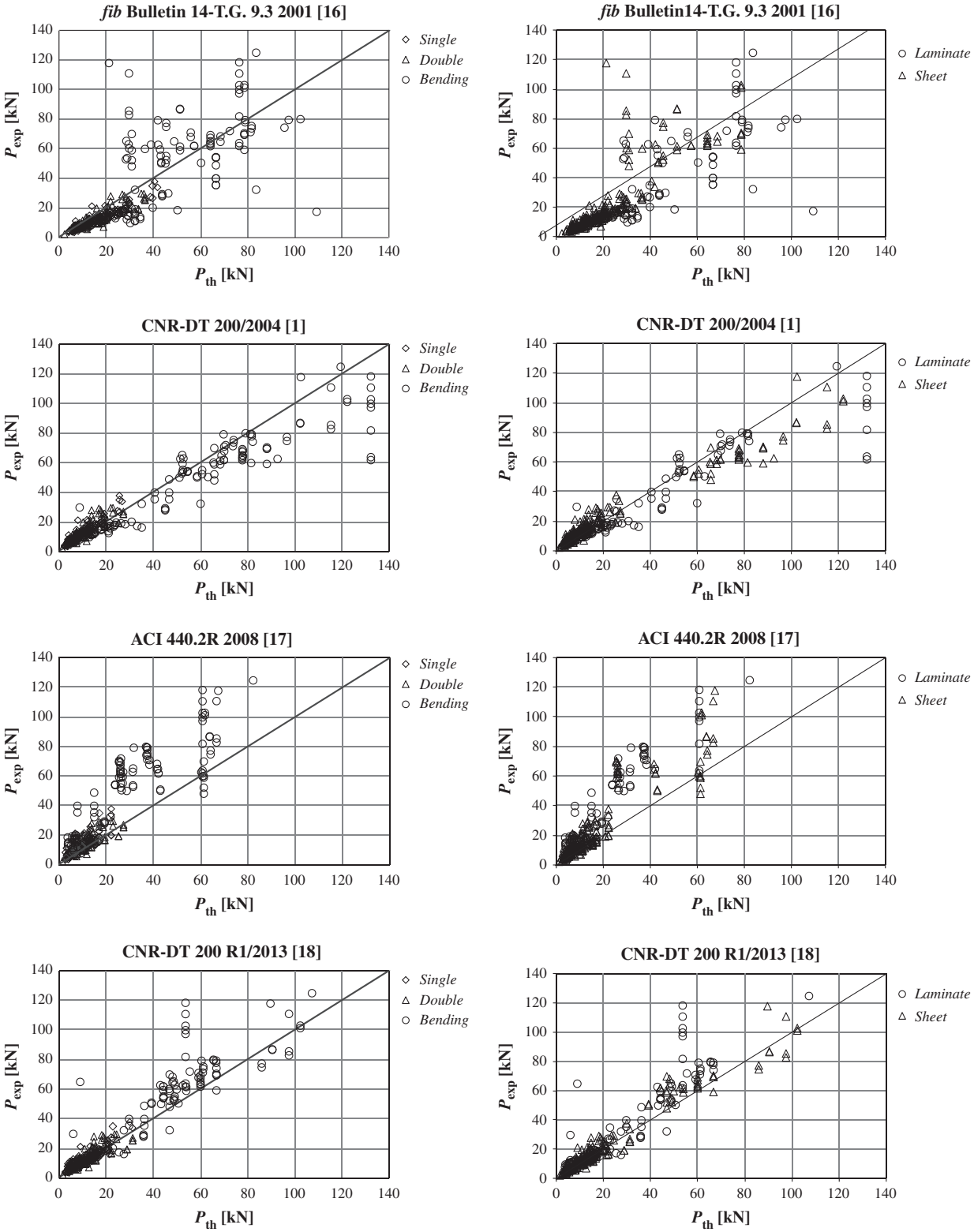

Fig. 2. Comparison between experimental and analytical values for various experimental setups (*Single*, *Double*, *Bending*), and different FRP composite material preparations (*Laminates*, *Sheets*).

the database was formed. For these reasons the analysis of the influence of the material preparation for a given test setup was not developed.

Considering the overall results without distinguishing test setups and material preparation, the statistical analysis shows that the analytical formulation of Camli and Binici [27] for the evalua-

Table 1
Results of the statistical analysis in terms of coefficient of variation *CoV* and average values *Avg*.

Analytical model	Single		Double		Bending		Sheet		Laminate		Sheet + Laminate	
	Avg	*CoV*	*Avg*	*CoV*	*Avg*	*CoV*	*Avg*	*CoV*	*Avg*	*CoV*	*Avg*	*CoV*
Van Gemert [19]	1.51	0.84	0.94	0.54	0.79	3.07	1.21	0.66	0.76	1.02	1.10	0.76
Tanaka [11]	1.75	1.20	1.40	0.70	–	–	1.88	1.00	1.96	2.54	1.77	1.21
Hiroyuki and Wu [20]	1.91	1.15	1.82	1.25	1.90	1.38	1.88	1.37	1.96	1.40	1.90	1.38
Maeda et al. [11]	0.97	0.24	1.05	0.32	1.34	0.91	1.09	0.56	1.07	0.44	1.09	0.53
Neubauer and Rostasy [21]	0.87	1.38	0.99	0.22	1.31	0.91	1.02	0.51	0.99	0.53	1.02	0.51
Khalifa et al. [22]	1.24	0.41	1.05	0.38	1.25	0.88	1.28	0.62	1.01	0.42	1.22	0.58
fib Bulletin 14-T.G. 9.3 [16]	0.84	0.23	0.85	0.26	1.10	0.72	0.93	0.44	0.87	0.41	0.91	0.43
Adhikary and Mutsuyoshi [23]	0.90	0.41	0.55	0.55	0.20	0.81	0.72	0.47	0.45	0.81	0.65	0.57
Chen and Teng [11]	1.47	1.38	1.66	0.75	2.21	1.88	1.71	1.11	1.72	1.13	1.71	1.12
De Lorenzis et al. [24]	0.67	0.36	0.72	0.34	0.88	0.60	0.75	0.45	0.70	0.42	0.74	0.44
Izumo [25]	0.85	0.39	0.69	0.62	0.10	0.98	0.74	0.52	0.07	0.93	0.62	0.61
Iso [25]	1.06	0.26	0.96	0.31	1.06	0.77	1.10	0.49	0.87	0.41	1.04	0.47
Sato [25]	0.73	0.36	0.85	0.53	0.50	0.81	0.76	0.47	0.44	0.73	0.68	0.54
Yang et al. [13]	1.14	0.30	1.04	0.35	1.34	0.91	1.22	0.58	1.09	0.43	1.18	0.55
CNR DT-200 [1]	1.42	0.52	1.34	0.52	0.94	0.33	1.34	0.50	1.03	0.39	1.26	0.47
Dai et al. [26]	0.61	0.41	0.67	0.38	0.86	0.59	0.70	0.47	0.66	0.45	0.69	0.46
Lu et al. [13]	1.00	0.18	1.17	0.32	1.55	1.14	1.18	0.64	1.18	0.62	1.18	0.63
Camli and Binici [27]	1.01	0.31	0.84	0.37	0.60	0.56	0.93	0.35	0.68	0.52	0.87	0.40
ACI 440.2R [17]	1.45	0.59	1.78	0.94	2.23	1.50	1.54	0.72	2.12	1.40	1.68	0.93
CNR DT-200 R1 [18]	1.30	0.44	1.22	0.42	1.26	0.77	1.23	0.36	1.41	0.91	1.28	0.55

tion of the FRP–concrete bond strength shows the smallest coefficient of variation, equal to 0.40.

5. Assessment of the effective bond length evaluation models

Twelve analytical models for the evaluation of the effective bond length were analysed comparing the experimental value, $l_{e,exp}$, with the theoretical provisions, $l_{e,th}$.

The following models for the effective bond length are considered:

fib Bulletin 14-T.G. 9.3 [16] – *CNR DT-200* [1] – *Neubauer and Rostàsy* [21]

The European [16], Italian [1], and Neubauer and Rostàsy [21] models propose the same formulation to compute the effective bond length for FRP strengthening:

$$l_e = \sqrt{\frac{E_f t_f}{2 f_{ctm}}} \tag{48}$$

ACI 440.2R [17]

The ACI 440.2R [17] defines the effective bond length, indicated as active bond length l_e, as the length over which the majority of the bond strength is maintained. This length is given by Eq. (49):

$$l_e = \frac{23,300}{(n_f t_f E_f)^{0.58}} \tag{49}$$

where n_f is the modular ratio of elasticity between FRP and concrete equal to E_f/E_c. It should be pointed out that in case of pure axial strengthening a bonded length equal to $2l_e$ is suggested in order to obtain the strain levels provided by Eq. (11).

CNR DT-200 R1 [18]

The CNR-DT 200 R1 [18] computes the effective bond length, named optimum bond length, according to Eqs. (50) and (51).

$$l_e = \min\left\{\frac{1}{\gamma_{Rd}\cdot f_{bd}}\sqrt{\frac{\pi^2\cdot E_f\cdot t_f\cdot \Gamma_{Fd}}{2}}, 200\right\} \tag{50}$$

$$f_{bd} = \frac{2\cdot \Gamma_{Fd}}{s_u} \tag{51}$$

where $s_u = 0.25$ is the ultimate slip between the FRP and the concrete support, and $\gamma_{Rd} = 1.25$ is a safety modification factor.

Maeda et al. [11] – *Khalifa et al.* [22]:Khalifa et al. [22] adopted the same model proposed by Maeda et al. [11]:

$$l_e = e^{6.13-0.580\ln E_f t_f} \tag{52}$$

Chen and Teng [11]:

$$l_e = \sqrt{\frac{E_f t_f}{\sqrt{f_c'}}} \tag{53}$$

Iso [25]:

$$l_e = 1.89(E_f t_f)^{0.4} \tag{54}$$

Sato [25]:

$$l_e = 0.125(E_f t_f)^{0.57} \tag{55}$$

Lu et al. [13]:

$$l_e = a + \frac{1}{2\lambda_1}\ln\frac{\lambda_1+\lambda_2\tan(\lambda_2 a)}{\lambda_1-\lambda_2\tan(\lambda_2 a)} \tag{56}$$

$$\lambda_1 = \sqrt{\frac{\tau_{max}}{s_0 E_f t_f}} \tag{57}$$

$$\lambda_2 = \sqrt{\frac{\tau_{max}}{(s_f - s_0) E_f t_f}} \tag{58}$$

$$a = \frac{1}{\lambda_2}\arcsin\left[0.99\sqrt{\frac{s_f - s_0}{s_f}}\right] \tag{59}$$

Table 2
Results of the statistical procedure to assess the FRP effective bond length analytical models.

Analytical model	CoV_e	StD_e	Avg_e	Overestimated (%)
CNR DT-200 [1]	0.17	0.17	0.97	73
fib Bulletin 14-T.G. 9.3 [16]				
Neubauer and Rostasy [21]				
Chen and Teng [11]	0.19	0.19	0.98	67
Camli and Binici [27]				
Sato [25]	0.41	0.16	0.62	100
Iso [25]	0.48	0.28	1.39	10
Lu et al. [13]	0.85	0.32	1.79	0
Maeda et al. [11]	4.74	3.90	3.75	2
Khalifa et al. [22]				
ACI 440.2R [17]	5.18	4.22	4.06	2
CNR DT-200 R1[18]	0.15	0.11	0.89	90

τ_{max} is the maximum local bond stress defined as:

$$\tau_{max} = \alpha_1 \beta_w f_t \quad (60)$$

where α_1 = 1.5, and s_0 is the corresponding local slip calculated as:

$$s_0 = 0.0195 \beta_w f_t \quad (61)$$

Camli and Binici [27]:

$$l_e = \sqrt{\frac{E_f t_f}{\sqrt{f_c}}} \quad (62)$$

Since there are few works in which the effective bond length was experimentally measured due to the practical difficulty of the procedure, the database was comprised of 48 specimens taken from [10,14,31–34,42]. The same statistical procedure adopted to assess the FRP–concrete bond strength models was carried out to assess the accuracy of the analytical models for the effective bond length. Table 2 summarises the results of the statistical analysis for each model (models proposing the same analytical formulation were gathered together). The value of the coefficient of variation, CoV_e, and the corresponding average value of the ratio between the

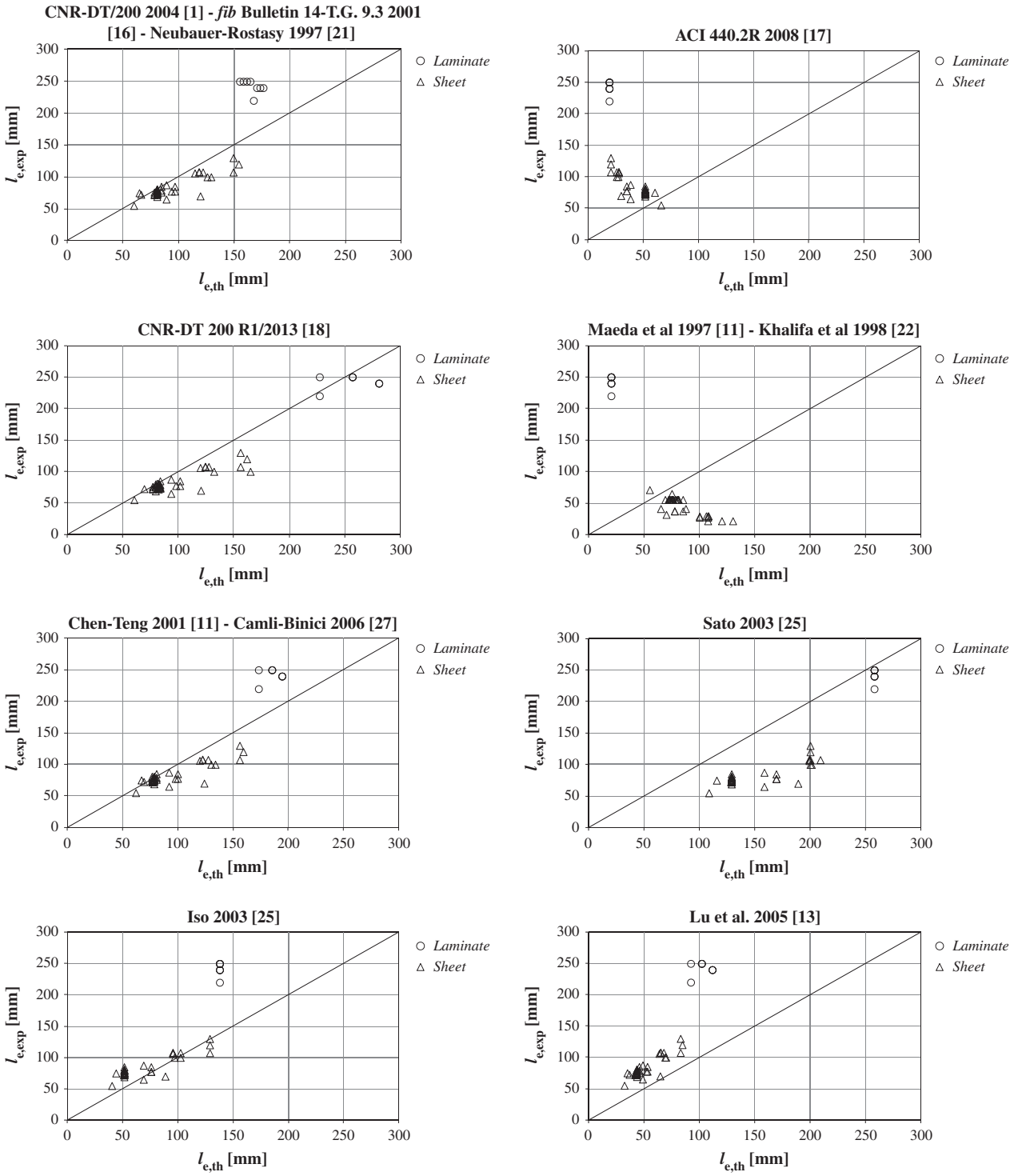

Fig. 3. Comparison between experimental and analytical effective bond length values for different material used (*Laminate*, *Sheet*).

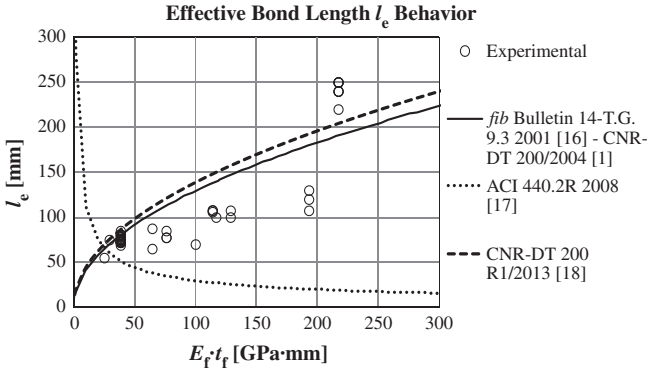

Fig. 4. Trend of the experimental and analytical effective bond length as the FRP stiffness increases for CNR-DT 200 2004 [1], *fib* Bulletin 14 T.G. 9.3 [16], ACI 440.2R [17], and CNR-DT 200 R1/2013 [18].

experimental and theoretical effective bond length, Avg_e, are reported. In addition, the standard deviation StD_e, and the percentage of the overestimated (not safe) effective bond length values are reported in Table 2 for each model. In this case the influence of the test setup and material preparation were not considered during the statistical analysis due to the small amount of available experimental data.

The most accurate result ($CoV_e = 0.15$) was obtained by the new version of the Italian guidelines CNR-DT 200 R1/2013 [18], which improves the model originally proposed by Neubauer and Rostasy [21] and adopted by the European guidelines [16] (Fig. 3).

The trend of the effective bond length as the FRP stiffness ($E_f\ t_f$) increases was studied and reported in Fig. 4 for CNR DT-200 [1], *fib* Bulletin 14 T.G. 9.3 [16], ACI 440.2R [17], and CNR DT-200 R1 [18]. Furthermore, in Fig. 4 it can be seen that the predictions are generally quite good for small values of the FRP stiffness, whereas become more scattered for higher values. The ACI 440.2R [17] model showed an opposite trend with respect to the other main formulations. This can be due to the fact that the American model is calibrated with few experimental observations and does not take into account the cohesive nature of the concrete substrate.

6. Conclusions

This paper presents a systematic assessment of twenty existing FRP–concrete bond strength models and twelve effective bond length formulations. The accuracy of each model was evaluated through computing the coefficient of variation of the ratio between the experimental results and the analytical provisions.

The assessment was performed using an experimental database consisting in 404 specimens for the bond strength models and 48 specimens for the effective bond length models. The influence of the test setup and material preparation on the accuracy of the considered bond strength models was investigated. The results show that the most diffused guidelines are sometimes unconservative in the estimation of the FRP–concrete bond strength.

The considered models seem to fit well the experimental results when compared to direct shear and double shear test setup, whereas the comparisons are typically more scattered and the analytical predictions become quite inaccurate when compared with full-scale bending tests. The reason is probably that existing bond strength models have been mainly calibrated with small databases mostly including single and double shear tests of few authors. However, it should be noted that the hypotheses on which the calculations of the bond strength of full-scale bending test are based, mainly relating to the assumption that the cross-sections of the beam remains plane, have to be taken into account for the interpretation of the results of this study. Based on this observation, a deep study of the parameters affecting the results in case of full-scale bending tests with respect to direct shear tests seems to be needed.

The formulations for the effective bond length are quite good for small values of the FRP stiffness ($E_f\ t_f$), whereas they become worse and, sometimes, unconservative as the FRP stiffness increases. Each analysed model for the effective bond length, as for the experimental results, shows an increasing trend of the effective bond length as FRP stiffness increases, except for the American guidelines that show an opposite trend and significant inaccuracy. Despite the practical difficult to experimentally measure the effective bond length, an increase of the database, in particular for high FRP stiffness, seems desirable for a better assessment of the existing analytical models.

The obtained results can give some insights for improving the existing models to fit better the experimental results and show the need of further investigations to properly understand FRP–concrete failure mechanism. Furthermore, this work could further stimulate the discussion in the scientific community with the aim of finding a shared test procedure for measuring key parameters for bond behaviour in RC elements strengthened with FRP composites.

Appendix A. Test database

The geometrical and mechanical characteristics of the tested specimens included in the database are reported in the following tables. Single shear tests and double shear tests are included in Tables A.1 and A.2, respectively. The characteristics of the RC beams tested in bending are shown in Table A.3, whereas

Table A.1
Geometrical and mechanical characteristics of the specimens tested using single shear test setup.

References	Specimen name	Concrete		FRP strengthening							Test results	
		b (mm)	f_c (MPa)	FRP	n	t_f (mm)	b_f (mm)	l_b (mm)	E_f (MPa)	f_f (MPa)	P_u (kN)	l_e (mm)
[10]	BN6	150	34.50	G_S	1	1.000	25.4	180.0	29,200	472	11.41	75
	BN20	150	34.50	G_S	2	2.000	25.4	320.0	29,200	472	21.40	100
	BN25	150	34.50	C_S	1	0.330	25.4	160.0	75,700	1014	8.50	55
	BN32	150	34.50	C_S	2	0.660	25.4	320.0	75,700	1014	15.10	70
[11]	C1	228.6	36.1	G_L	1	1.016	25.4	76.2	1,08,470	1655	8.46	–
	C2	228.6	47.1	G_L	1	1.016	25.4	76.2	1,08,470	1655	9.93	–
	C3	228.6	47.1	G_L	1	1.016	25.4	76.2	1,08,470	1655	10.64	–
	C4	228.6	47.1	G_L	1	1.016	25.4	76.2	1,08,470	1655	10.64	–
	C5	228.6	43.6	G_L	1	1.016	25.4	76.2	1,08,470	1655	10.53	–
	C6	228.6	43.6	G_L	1	1.016	25.4	76.2	1,08,470	1655	8.96	–

(*continued on next page*)

Table A.1 (*continued*)

References	Specimen name	Concrete		FRP strengthening							Test results	
		b (mm)	f_c (MPa)	FRP	n	t_f (mm)	b_f (mm)	l_b (mm)	E_f (MPa)	f_f (MPa)	P_u (kN)	l_e (mm)
	C7	228.6	43.6	G_L	1	1.016	25.4	76.2	1,08,470	1655	9.61	–
	C8	228.6	43.6	G_L	1	1.016	25.4	76.2	1,08,470	1655	10.52	–
	C9	228.6	43.6	G_L	1	1.016	25.4	76.2	1,08,470	1655	11.20	–
	C10	228.6	24	G_L	1	1.016	25.4	76.2	1,08,470	1655	9.87	–
	C11	228.6	28.9	G_L	1	1.016	25.4	76.2	1,08,470	1655	9.34	–
	C12	228.6	43.7	G_L	1	1.016	25.4	76.2	1,08,470	1655	11.20	–
	C13	228.6	36.4	G_L	1	1.016	25.4	50.8	1,08,470	1655	8.09	–
	C14	228.6	36.4	G_L	1	1.016	25.4	101.6	1,08,470	1655	12.81	–
	C15	152.4	36.4	G_L	1	1.016	25.4	152.4	1,08,470	1655	11.92	–
	C16	152.4	36.4	G_L	1	1.016	25.4	203.2	1,08,470	1655	11.57	–
	C100 50A	200	54.2	C_L	1	1.250	50	100.0	1,70,000	2497	17.30	–
	C200 50A	200	59.8	C_L	1	1.250	50	200.0	1,70,000	2497	27.50	–
	C300 50A	200	65.8	C_L	1	1.250	50	300.0	1,70,000	2497	35.10	–
	C400 50A	200	65.8	C_L	1	1.250	50	400.0	1,70,000	2497	26.90	–
[28]	I-1	150	23.0	C_S	1	0.165	25	75.0	2,56,000	4114	4.75	–
	I-2	150	23.0	C_S	1	0.165	25	85.0	2,56,000	4114	5.69	–
	I-3	150	23.0	C_S	1	0.165	25	95.0	2,56,000	4114	5.76	–
	I-4	150	23.0	C_S	1	0.165	25	95.0	2,56,000	4114	5.76	–
	I-5	150	23.0	C_S	1	0.165	25	95.0	2,56,000	4114	6.17	–
	I-6	150	23.0	C_S	1	0.165	25	115.0	2,56,000	4114	5.96	–
	I-7	150	23.0	C_S	1	0.165	25	145.0	2,56,000	4114	5.95	–
	I-8	150	23.0	C_S	1	0.165	25	190.0	2,56,000	4114	6.68	–
	I-9	150	23.0	C_S	1	0.165	25	190.0	2,56,000	4114	6.35	–
	I-10	150	23.0	C_S	1	0.165	25	95.0	2,56,000	4114	6.17	–
	I-11	150	23.0	C_S	1	0.165	25	75.0	2,56,000	4114	5.72	–
	I-12	150	23.0	C_S	1	0.165	25	85.0	2,56,000	4114	6.00	–
	I-13	150	23.0	C_S	1	0.165	25	95.0	2,56,000	4114	6.14	–
	I-14	150	23.0	C_S	1	0.165	25	115.0	2,56,000	4114	6.19	–
	I-15	150	23.0	C_S	1	0.165	25	145.0	2,56,000	4114	6.27	–
	I-16	150	23.0	C_S	1	0.165	25	190.0	2,56,000	4114	7.03	–
	II-1	150	22.9	C_S	1	0.165	25	95.0	2,56,000	4114	5.20	–
	II-2	150	22.9	C_S	1	0.165	25	95.0	2,56,000	4114	6.75	–
	II-3	150	22.9	C_S	1	0.165	25	95.0	2,56,000	4114	5.51	–
	II-4	150	22.9	C_S	1	0.165	25	190	2,56,000	4114	7.02	–
	II-5	150	22.9	C_S	1	0.165	25	190.0	2,56,000	4114	7.07	–
	II-6	150	22.9	C_S	1	0.165	25	190.0	2,56,000	4114	6.98	–
	III-1	150	27.1	C_S	1	0.165	25	100.0	2,56,000	4114	5.94	–
	III-2	150	27.1	C_S	1	0.165	50	100.0	2,56,000	4114	11.66	–
	III-3	150	27.1	C_S	1	0.165	75	100.0	2,56,000	4114	14.63	–
	III-4	150	27.1	C_S	1	0.165	100	100.0	2,56,000	4114	19.07	–
	III-5	100	27.1	C_S	1	0.165	85	100.0	2,56,000	4114	15.08	–
	III-6	100	27.1	C_S	1	0.165	100	100.0	2,56,000	4114	15.75	–
	III-7	100	27.1	G_L	1	1.270	25.3	100.0	22,500	351	4.78	–
	III-8	100	27.1	G_L	1	1.270	50.6	100.0	22,500	351	8.02	–
	IV-1	150	18.9	C_S	1	0.165	25	95.0	2,56,000	4114	5.86	–
	IV-2	150	18.9	C_S	1	0.165	25	95.0	2,56,000	4114	5.90	–
	IV-3	150	19.8	C_S	1	0.165	25	95.0	2,56,000	4114	5.43	–
	IV-4	150	19.8	C_S	1	0.165	25	95.0	2,56,000	4114	5.76	–
	IV-5	150	18.9	C_S	1	0.165	25	95.0	2,56,000	4114	5.00	–
	IV-6	150	19.8	C_S	1	0.165	25	95.0	2,56,000	4114	7.08	–
	IV-7	150	18.9	C_S	1	0.165	25	95.0	2,56,000	4114	5.50	–
	IV-8	150	19.8	C_S	1	0.165	25	95.0	2,56,000	4114	5.93	–
	IV-9	150	18.9	C_S	1	0.165	25	95.0	2,56,000	4114	5.38	–
	IV-10	150	19.8	C_S	1	0.165	25	95.0	2,56,000	4114	6.60	–
	IV-11	150	18.9	C_S	1	0.165	25	95.0	2,56,000	4114	5.51	–
	IV-12	150	19.8	C_S	1	0.165	25	95.0	2,56,000	4114	5.67	–
	IV-13	150	18.9	C_S	1	0.165	25	95.0	2,56,000	4114	6.31	–
	IV-14	150	19.8	C_S	1	0.165	25	95.0	2,56,000	4114	6.19	–
	V-1	150	21.1	C_S	1	0.165	15	95.0	2,56,000	4114	3.81	–
	V-2	150	21.1	C_S	1	0.165	15	95.0	2,56,000	4114	4.41	–
	V-3	150	21.1	C_S	1	0.165	25	95.0	2,56,000	4114	6.26	–
	V-4	150	21.1	C_S	1	0.165	50	95.0	2,56,000	4114	12.22	–
	V-5	150	21.1	C_S	1	0.165	75	95.0	2,56,000	4114	14.29	–
	V-6	150	21.1	C_S	1	0.165	100	95.0	2,56,000	4114	15.58	–
	V-7	100	21.1	C_S	1	0.165	80	95.0	2,56,000	4114	14.27	–
	V-8	100	21.1	C_S	1	0.165	80	95.0	2,56,000	4114	13.78	–
	V-9	100	21.1	C_S	1	0.165	90	95.0	2,56,000	4114	13.56	–
	V-10	100	21.1	C_S	1	0.165	90	95.0	2,56,000	4114	15.66	–
	V-11	100	21.1	C_S	1	0.165	100	95.0	2,56,000	4114	15.57	–
	V-12	100	21.1	C_S	1	0.165	100	95.0	2,56,000	4114	17.43	–
	VI-1	150	21.9	C_S	1	0.165	25	95.0	2,56,000	4114	6.01	–
	VI-2	150	21.9	C_S	1	0.165	25	95.0	2,56,000	4114	5.85	–
	VI-3	150	21.9	C_S	1	0.165	25	145.0	2,56,000	4114	5.76	–
	VI-4	150	21.9	C_S	1	0.165	25	145.0	2,56,000	4114	5.73	–

Table A.1 (*continued*)

References	Specimen name	Concrete		FRP strengthening							Test results	
		b (mm)	f_c (MPa)	FRP	n	t_f (mm)	b_f (mm)	l_b (mm)	E_f (MPa)	f_f (MPa)	P_u (kN)	l_e (mm)
	VI-5	150	21.9	C_S	1	0.165	25	190.0	2,56,000	4114	5.56	–
	VI-6	150	21.9	C_S	1	0.165	25	190.0	2,56,000	4114	5.58	–
	VI-7	150	21.9	C_S	1	0.165	25	240.0	2,56,000	4114	5.91	–
	VI-8	150	21.9	C_S	1	0.165	25	240.0	2,56,000	4114	5.05	–
	VII-1	150	24.9	C_S	1	0.165	25	95.0	2,56,000	4114	6.8	–
	VII-2	150	24.9	C_S	1	0.165	25	95.0	2,56,000	4114	6.62	–
	VII-3	150	24.9	C_S	1	0.165	25	145.0	2,56,000	4114	7.33	–
	VII-4	150	24.9	C_S	1	0.165	25	145.0	2,56,000	4114	6.49	–
	VII-5	150	24.9	C_S	1	0.165	25	190.0	2,56,000	4114	7.07	–
	VII-6	150	24.9	C_S	1	0.165	25	190	2,56,000	4114	7.44	–
	VII-7	150	24.9	C_S	1	0.165	25	240.0	2,56,000	4114	7.16	–
	VII-8	150	24.9	C_S	1	0.165	25	240.0	2,56,000	4114	6.24	–
[13]	1-11	100	2.86	C_S	1	0.167	40	100.0	2,30,000	3481	8.75	–
	1-12	100	2.74	C_S	1	0.167	40	100.0	2,30,000	3481	8.85	–
	1-21	100	2.86	C_S	1	0.167	40	200.0	2,30,000	3481	9.30	–
	1-22	100	2.74	C_S	1	0.167	40	200.0	2,30,000	3481	8.50	–
	1-31	100	2.86	C_S	1	0.167	40	300.0	2,30,000	3481	9.30	–
	1-32	100	2.74	C_S	1	0.167	40	300.0	2,30,000	3481	8.30	–
	1-41	100	2.86	C_S	1	0.167	40	500.0	2,30,000	3481	8.05	–
	1-42	100	2.86	C_S	1	0.167	40	500.0	2,30,000	3481	8.05	–
	1-51	100	2.73	C_S	1	0.167	40	500.0	2,30,000	3481	8.45	–
	1-52	100	2.73	C_S	1	0.167	40	500.0	2,30,000	3481	7.30	–
	2-11	100	2.64	C_S	1	0.167	40	100.0	2,30,000	3481	8.75	–
	2-12	100	2.64	C_S	1	0.167	40	100.0	2,30,000	3481	8.85	–
	2-13	100	2.71	C_S	1	0.167	40	100.0	2,30,000	3481	7.75	–
	2-14	100	2.71	C_S	1	0.167	40	100.0	2,30,000	3481	7.65	–
	2-15	100	2.61	C_S	1	0.167	40	100.0	2,30,000	3481	9.00	–
	2-21	100	2.64	C_S	1	0.334	40	100.0	2,30,000	3481	12.00	–
	2-22	100	2.64	C_S	1	0.334	40	100.0	2,30,000	3481	10.80	–
	2-31	100	2.64	C_S	1	0.501	40	100.0	2,30,000	3481	12.65	–
	2-32	100	2.64	C_S	1	0.501	40	100.0	2,30,000	3481	14.35	–
	2-41	100	2.61	C_S	1	0.165	40	100.0	3,73,000	2942	11.55	–
	2-42	100	2.61	C_S	1	0.165	40	100.0	3,73,000	2942	11.00	–
	2-51	100	2.71	C_S	1	0.167	40	100.0	2,30,000	3481	9.85	–
	2-52	100	2.71	C_S	1	0.167	40	100.0	2,30,000	3481	9.50	–
	2-61	100	2.71	C_S	1	0.167	40	100.0	2,30,000	3481	8.80	–
	2-62	100	2.71	C_S	1	0.167	40	100.0	2,30,000	3481	9.25	–
	2-71	100	2.71	C_S	1	0.167	40	100.0	2,30,000	3481	7.65	–
	2-72	100	2.71	C_S	1	0.167	40	100.0	2,30,000	3481	6.80	–
	2-81	100	3.87	C_S	1	0.167	40	100.0	2,30,000	3481	7.75	–
	2-82	100	3.87	C_S	1	0.167	40	100.0	2,30,000	3481	8.08	–
	2-91	100	2.61	C_S	1	0.167	40	100.0	2,30,000	3481	6.75	–
	2-92	100	2.61	C_S	1	0.167	40	100.0	2,30,000	3481	6.80	–
	2-101	100	2.64	C_S	1	0.111	40	100.0	2,30,000	3481	7.70	–
	2-102	100	2.71	C_S	1	0.111	40	100.0	2,30,000	3481	6.95	–
	NJ2	150	2.08	C_S	1	0.083	100	100.0	2,40,000	3550	11.00	–
	NJ3	150	2.08	C_S	1	0.083	100	150.0	2,40,000	3550	11.25	–
	NJ4	150	2.87	C_S	1	0.083	100	100.0	2,40,000	3550	12.50	–
	NJ5	150	2.87	C_S	1	0.083	100	150.0	2,40,000	3550	12.25	–
	NJ6	150	2.87	C_S	1	0.083	100	150.0	2,40,000	3550	12.75	–
	Ueda_B1	500	2.64	C_S	1	0.110	100	200.0	2,30,000	3479	20.60	–
	Ueda_B2	500	3.49	C_S	1	0.330	100	200.0	2,30,000	3479	38.00	–
	Ueda_B3	500	3.71	C_S	1	0.330	100	200.0	2,30,000	3479	34.10	–
	S-CFS-400-25a	100	4.21	C_S	1	0.222	40	250.0	2,30,000	4200	15.40	–
	S-CFS-400-25b	100	4.21	C_S	1	0.222	40	250.0	2,30,000	4200	13.90	–
	S-CFS-400-25c	100	4.21	C_S	1	0.222	40	250.0	2,30,000	4200	13.00	–
	S-CFM-300-25a	100	4.21	C_S	1	0.167	40	250.0	3,90,000	4400	12.00	–
	S-CFM-300-25b	100	4.21	C_S	1	0.167	40	250.0	3,90,000	4400	11.90	–
	S-CFM-900-25a	100	4.21	C_S	1	0.500	40	250.0	3,90,000	4400	25.90	–
	S-CFM-900-25b	100	4.21	C_S	1	0.5	40	250	3,90,000	4400	23.40	–
	S-CFM-900-25c	100	4.21	C_S	1	0.500	40	250.0	3,90,000	4400	23.70	–
	DLUT15-2G	150	2.50	C_S	1	0.507	20	150.0	83,000	3271	5.81	–
	DLUT15-5G	150	2.50	C_S	1	0.507	50	150.0	83,000	3271	10.60	–
	DLUT15-7G	150	2.50	C_S	1	0.507	80	150.0	83,000	3271	18.23	–
	DLUT30-1G	150	3.22	C_S	1	0.507	20	100.0	83,000	3271	4.63	–
	DLUT30-2G	150	3.22	C_S	1	0.507	20	150.0	83,000	3271	5.77	–
	DLUT30-3G	150	3.22	C_S	1	0.507	50	60.0	83,000	3271	9.42	–
	DLUT30-4G	150	3.22	C_S	1	0.507	50	100.0	83,000	3271	11.03	–
	DLUT30-6G	150	3.22	C_S	1	0.507	50	150.0	83,000	3271	11.80	–
	DLUT30-7G	150	3.22	C_S	1	0.507	80	100.0	83,000	3271	14.65	–
	DLUT30-8G	150	3.22	C_S	1	0.507	80	150.0	83,000	3271	16.44	–
	DLUT50-1G	150	3.60	C_S	1	0.507	20	100.0	83,000	3271	5.99	–
	DLUT50-2G	150	3.60	C_S	1	0.507	20	150.0	83,000	3271	5.90	–

(*continued on next page*)

Table A.1 (*continued*)

References	Specimen name	Concrete		FRP strengthening							Test results	
		b (mm)	f_c (MPa)	FRP	n	t_f (mm)	b_f (mm)	l_b (mm)	E_f (MPa)	f_f (MPa)	P_u (kN)	l_e (mm)
	DLUT50-4G	150	3.60	C_S	1	0.507	50	100.0	83,000	3271	9.84	–
	DLUT50-5G	150	3.60	C_S	1	0.507	50	150.0	83,000	3271	12.28	–
	DLUT50-6G	150	3.60	C_S	1	0.507	80	100.0	83,000	3271	14.02	–
	DLUT50-7G	150	3.60	C_S	1	0.507	80	150.0	83,000	3271	16.71	–
	DLUT15-2C	150	2.50	C_S	1	0.330	20	150.0	2,07,000	3890	5.48	–
	DLUT15-5C	150	2.50	C_S	1	0.330	50	150.0	2,07,000	3890	10.02	–
	DLUT15-7C	150	2.50	C_S	1	0.330	80	150.0	2,07,000	3890	19.27	–
	DLUT30-1C	150	3.22	C_S	1	0.330	20	100.0	2,07,000	3890	5.54	–
	DLUT30-2C	150	3.22	C_S	1	0.330	20	150.0	2,07,000	3890	4.61	–
	DLUT30-4C	150	3.22	C_S	1	0.330	50	100.0	2,07,000	3890	11.08	–
	DLUT30-5C	150	3.22	C_S	1	0.330	50	100.0	2,07,000	3890	16.10	–
	DLUT30-6C	150	3.22	C_S	1	0.330	50	150.0	2,07,000	3890	21.71	–
	DLUT30-7C	150	3.22	C_S	1	0.330	80	100.0	2,07,000	3890	22.64	–
	DLUT50-1C	150	3.60	C_S	1	0.330	20	100.0	2,07,000	3890	5.78	–
	DLUT50-4C	150	3.60	C_S	1	0.330	50	100.0	2,07,000	3890	12.95	–
	DLUT50-5C	150	3.60	C_S	1	0.330	50	150.0	2,07,000	3890	16.72	–
	DLUT50-6C	150	3.60	C_S	1	0.330	80	100.0	2,07,000	3890	16.24	–
	DLUT50-7C	150	3.60	C_S	1	0.330	80	150.0	2,07,000	3890	22.80	–
	D-AR-280-30a	100	61.30	C_L	1	1.000	100	300.0	23,900	4400	12.75	–
	D-AR-280-30b	100	61.30	C_L	1	1.000.	100	300.0	23,900	4400	12.85	–
	D-AR-280-30c	100	61.30	C_L	1	1.000	100	300.0	23,900	4400	11.90	–
[29]	I-1	200	17.00	C_S	3	0.165	50	100.0	110,000	660	7.56	–
	I-2	200	17.00	C_S	4	0.165	50	100.0	110,000	660	9.29	–
	I-3	200	17.00	C_S	5	0.165	50	100.0	110,000	660	11.64	–
	I-4	200	17.00	C_S	6	0.165	50	100.0	110,000	660	12.86	–
	II-1	200	46.00	C_S	3	0.165	50	100.0	110,000	660	12.55	–
	II-2	200	46.00	C_S	4	0.165	50	100.0	110,000	660	14.25	–
	II-3	200	46.00	C_S	5	0.165	50	100.0	110,000	660	17.72	–
	II-4	200	46.00	C_S	6	0.165	50	100.0	110,000	660	18.86	–
	III-1	200	61.50	C_S	3	0.165	50	100.0	110,000	660	13.24	–
	III-2	200	61.50	C_S	4	0.165	50	100.0	110,000	660	15.17	–
	III-3	200	61.50	C_S	5	0.165	50	100.0	110,000	660	18.86	–
	III-4	200	61.50	C_S	6	0.165	50	100.0	110,000	660	19.03	–
[30]	C150_100_1	150	21.58	C_S	1	0.165	100	150.0	2,30,000	4800	18.97	–
	C150_100_2	150	21.58	C_S	1	0.165	100	150.0	2,30,000	4800	16.51	–
	C150_100_3	150	21.58	C_S	1	0.165	100	150.0	2,30,000	4800	14.26	–
	C150_100_4	150	21.58	C_S	1	0.165	100	150	2,30,000	4800	15.10	–
	C150_100_2L_1	150	21.58	C_S	2	0.165	100	100.0	2,30,000	4800	20.12	–
	C150_100_2L_2	150	21.58	C_S	2	0.165	100	100.0	2,30,000	4800	19.87	–
	C100_100_1	150	21.58	C_S	1	0.165	100	100.0	2,30,000	4800	13.63	–
	C100_100_2	150	21.58	C_S	1	0.165	100	100.0	2,30,000	4800	13.36	–
	C150_50_1	150	21.58	C_S	1	0.165	50	150.0	2,30,000	4800	9.80	–
	C150_50_2	150	21.58	C_S	1	0.165	50	150.0	2,30,000	4800	6.00	–
	C150_50_3	150	21.58	C_S	1	0.165	50	150.0	2,30,000	4800	7.00	–
	C150_50_2L_1	150	21.58	C_S	2	0.165	50	150.0	2,30,000	4800	11.44	–
	C150_50_2L_2	150	21.58	C_S	2	0.165	50	150.0	2,30,000	4800	9.97	–
	C150_50_2L_3	150	21.58	C_S	2	0.165	50	150.0	2,30,000	4800	10.04	–
	C150_25_1	150	21.58	C_S	1	0.165	25	150.0	2,30,000	4800	6.00	–
	C150_25_2	150	21.58	C_S	1	0.165	25	150.0	2,30,000	4800	3.70	–
	C150_25_3	150	21.58	C_S	1	0.165	25	150.0	2,30,000	4800	5.80	–
	C150_75_1	150	21.58	C_S	1	0.165	75	150.0	2,30,000	4800	14.40	–
	C150_75_2	150	21.58	C_S	1	0.165	75	150.0	2,30,000	4800	12.96	–
[31]	W-1	125	39.00	C_S	1	0.167	46	152.0	2,30,000	3830	12.90	80
	W-2	125	39.00	C_S	1	0.167	46	152.0	2,30,000	3830	12.05	76
	W-3	125	39.00	C_S	1	0.167	46	152.0	2,30,000	3830	13.20	75
	W-4	125	39.00	C_S	1	0.167	38	152.0	2,30,000	3830	10.09	81
	W-5	125	39.00	C_S	1	0.167	38	152.0	2,30,000	3830	10.02	73
	W-6	125	39.00	C_S	1	0.167	25	152.0	2,30,000	3830	5.54	80
	W-7	125	39.00	C_S	1	0.167	25	152.0	2,30,000	3830	5.44	76
	W-8	125	39.00	C_S	1	0.167	25	152.0	2,30,000	3830	5.36	69
	W-9	125	39.00	C_S	1	0.167	19	152.0	2,30,000	3830	4.27	75
	W-10	125	39.00	C_S	1	0.167	19	152.0	2,30,000	3830	4.05	78
[32]	Test 7	52	31.00	C_S	1	0.167	25	152.0	2,30,000	3830	8.65	74
	Test 8	52	31.00	C_S	1	0.167	25	152.0	2,30,000	3830	6.89	73
	Test 12	52	31.00	C_S	1	0.167	22	152.0	2,30,000	3830	7.44	72
	Test 13	52	31.00	C_S	1	0.167	22	152.0	2,30,000	3830	7.17	81
	DS_2	52	31.00	C_S	1	0.167	20	152.0	2,30,000	3830	6.15	75
	DS_3	52	31.00	C_S	1	0.167	20	152.0	2,30,000	3830	6.45	78
[33]	DS-S1	125	35.00	C_S	1	0.167	25	152.0	2,30,000	3830	8.04	79
	DS-S2	125	35.00	C_S	1	0.167	25	152.0	2,30,000	3830	7.74	76
	DS-S3	125	35.00	C_S	1	0.167	25	152.0	2,30,000	3830	7.01	85
[34]	DS-ST_1	125	35.00	C_S	1	0.167	25	152.0	2,30,000	3830	5.80	76
	DS-ST_2	125	35.00	C_S	1	0.167	25	152.0	2,30,000	3830	6.30	72
	DS-ST_3	125	35.00	C_S	1	0.167	25	152.0	2,30,000	3830	6.00	73

Table A.2
Geometrical and mechanical characteristics of the specimens tested using double shear test setup.

References	Specimen name	Concrete		FRP strengthening							Test results	
		b (mm)	f_c (MPa)	FRP	n	t_f (mm)	b_f (mm)	l_b (mm)	E_f (MPa)	f_f (MPa)	P_u (kN)	l_e (mm)
[13]	Ueda_A1	100	2.55	C_S	1	0.110	50	75	2,30,000	3479	6.25	–
	Ueda_A2	100	3.48	C_S	1	0.110	50	150	2,30,000	3479	9.20	–
	Ueda_A3	100	3.48	C_S	1	0.110	50	300	2,30,000	3479	11.95	–
	Ueda_A4	100	3.60	C_S	1	0.220	50	75	2,30,000	3479	10.00	–
	Ueda_A5	100	3.56	C_S	1	0.110	50	150	2,30,000	3479	7.30	–
	Ueda_A6	100	3.56	C_S	1	0.165	50	65	3,72,000	2940	9.55	–
	Ueda_A7	100	3.57	C_S	1	0.220	50	150	2,30,000	3479	16.25	–
	Ueda_A8	100	3.57	C_S	1	0.110	50	700	2,30,000	3479	11.00	–
	Ueda_A9	100	3.43	C_S	1	0.110	50	150	2,30,000	3479	10.00	–
	Ueda_A10	100	2.59	C_S	1	0.110	10	150	2,30,000	3479	2.40	–
	Ueda_A11	100	2.59	C_S	1	0.110	20	150	2,30,000	3479	5.35	–
	Ueda_A12	100	2.59	C_S	1	0.330	20	150	2,30,000	3479	9.25	–
	Ueda_A13	100	2.64	C_S	1	0.550	20	150	2,30,000	3479	11.75	–
	D-CFS-150-30a	100	3.71	C_S	1	0.083	100	300	2,30,000	4200	12.20	–
	D-CFS-150-30b	100	4.21	C_S	1	0.083	100	300	2,30,000	4200	11.80	–
	D-CFS-150-30c	100	4.21	C_S	1	0.083	100	300	2,30,000	4200	12.25	–
	D-CFS-300-30a	100	4.21	C_S	1	0.167	100	300	2,30,000	4200	18.90	–
	D-CFS-300-30b	100	4.21	C_S	1	0.167	100	300	2,30,000	4200	16.95	–
	D-CFS-300-30c	100	4.21	C_S	1	0.167	100	300	2,30,000	4200	16.65	–
	D-CFS-600-30a	100	4.21	C_S	1	0.333	100	300	2,30,000	4200	25.65	–
	D-CFS-600-30b	100	4.21	C_S	1	0.333	100	300	2,30,000	4200	25.35	–
	D-CFS-600-30c	100	4.21	C_S	1	0.333	100	300	2,30,000	4200	27.25	–
	D-CFM-300-30a	100	4.21	C_S	1	0.167	100	300	3,90,000	4400	19.50	–
	D-CFM-300-30b	100	4.21	C_S	1	0.167	100	300	3,90,000	4400	19.50	–
	PG1-11	100	2.90	C_S	1	0.169	50	130	97,000	2777	7.78	–
	PG1-12	100	2.90	C_S	1	0.169	50	130	97,000	2777	9.19	–
	PG1-1W1	100	2.90	C_S	1	0.169	75	130	97,000	2777	10.11	–
	PG1-1W2	100	2.90	C_S	1	0.169	75	130	97,000	2777	13.95	–
	PG1-1L11	100	2.90	C_S	1	0.169	50	100	97,000	2777	6.87	–
	PG1-1L12	100	2.90	C_S	1	0.169	50	100	97,000	2777	9.20	–
	PG1-1L21	100	2.90	C_S	1	0.169	50	70	97,000	2777	6.46	–
	PG1-1L22	100	2.90	C_S	1	0.169	50	70	97,000	2777	6.66	–
	PG1-21	100	2.90	C_S	1	0.338	50	130	97,000	2777	10.49	–
	PG1-22	100	2.90	C_S	1	0.338	50	130	97,000	2777	11.43	–
	PG1-1C1	100	2.90	C_S	1	0.111	50	130	2,35,000	3500	7.97	–
	PG1-1C2	100	2.90	C_S	1	0.111	50	130	2,35,000	3500	9.19	–
	M1	100	40.80	C_S	1	0.110	50	75	2,30,000	3500	5.80	–
	M2	100	40.80	C_S	1	0.110	50	150	2,30,000	3500	9.20	–
	M3	100	43.30	C_S	1	0.110	50	300	2,30,000	3500	11.95	–
	M4	100	42.40	C_S	1	0.165	50	75	2,30,000	3500	10.00	–
	M5	100	42.40	C_S	1	0.165	50	150	2,30,000	3500	7.30	–
	M6	100	42.70	C_S	1	0.220	50	65	2,30,000	3500	9.55	–
	M7	100	42.70	C_S	1	0.220	50	150	2,30,000	3500	16.25	–
	M8	100	44.70	C_S	1	0.11	50	700	2,30,000	3500	10.00	–
[14]	S1C1a	100	55.00	C_S	1	0.165	50	200	2,30,000	3430	19.98	72.5
	S1C5a	100	55.00	C_S	1	0.165	50	200	3,90,000	3000	21.33	–
	S1C5b	100	55.00	C_S	1	0.165	50	200	3,90,000	3000	16.76	–
	S1C5c	100	50.00	C_S	1	0.165	50	280	3,90,000	3000	18.79	87.5
	S1C5d	100	50.00	C_S	1	0.165	50	200	3,90,000	3000	12.11	65.0
	S2C1a	100	55.00	C_S	2	0.165	50	200	2,30,000	3430	21.74	77.5
	S2C1b	100	50.00	C_S	2	0.165	50	200	2,30,000	3430	24.67	85.0
	S2C1c	100	50.00	C_S	2	0.165	50	280	2,30,000	3430	28.21	77.5
	S3C1a	100	55.00	C_S	3	0.165	50	200	2,30,000	3430	28.44	106.0
	S3C1b	100	50.00	C_S	3	0.165	50	200	2,30,000	3430	25.99	108.0
	S3C1c	100	50.00	C_S	3	0.165	50	200	2,30,000	3430	29.33	107.5
	S2C5a	100	55.00	C_S	2	0.165	50	280	3,90,000	3000	25.55	107.5
	S2C5b	100	50.00	C_S	2	0.165	50	200	3,90,000	3000	27.10	100.0
	S3C5a	100	55.00	C_S	3	0.165	50	200	3,90,000	3000	26.41	107.5
	S3C5b	100	55.00	C_S	3	0.165	50	200	3,90,000	3000	29.73	130.0
	S3C5c	100	50.00	C_S	3	0.165	50	200	3,90,000	3000	29.79	120.0

Table A.4 report the corresponding characteristics of the FRP strengthening used. The following notation is adopted:

FRP = strengthening material preparation, C_S = carbon post-impregnated sheets, G_S = glass post-impregnated sheets, C_L = carbon pre-impregnated laminates, G_L = glass pre-impregnated laminates; f_f = FRP tensile strength; n = number of FRP layers; t_f = thickness of one FRP layer; P_u = experimental maximum load; h = height of the RC beam; A_s = area of the reinforcing steel in tension; A'_s = area of the reinforcing steel in compression; d_s = depth of the reinforcing steel in tension; d'_s = depth of the reinforcing steel in compression; f_y = yielding strength of the steel in tension; f'_y = yielding strength of the steel in compression. All the remaining symbols were explained into the text.

Table A.3
Geometrical and mechanical characteristics of the RC beams tested in bending.

References	Specimen name	Concrete			Steel reinforcement					
		b (mm)	h (mm)	f_c (MPa)	A_s (mm^2)	A'_s (mm^2)	d_s (mm)	d'_s (mm)	f_y (MPa)	f'_y (MPa)
[35]	AF.2	125	225	41.00	157.1	56.5	202.5	22.5	568	553
	AF.2-1	125	225	41.00	157.1	56.5	202.5	22.5	568	553
	AF.4	125	225	41.00	157.1	56.5	202.5	22.5	568	553
	DF.1	125	225	42.00	157.1	56.5	202.5	22.5	568	553
[36]	F5	155	240	80	339.3	226.2	203	37	532	532
	F6	155	240	80	339.3	226.2	203	37	532	532
	F7	155	240	80	339.3	226.2	203	37	532	532
	F8	155	240	80	339.3	226.2	203	37	532	532
	F9	155	240	80	339.3	226.2	203	37	532	532
	F10	155	240	80	339.3	226.2	203	37	532	532
[37]	A4	200	150	54.00	157.1	100.5	120	30	575	575
	A5	200	150	54.00	157.1	100.5	120	30	575	575
	A6	200	150	54.00	157.1	100.5	120	30	575	575
	A7	200	150	54.00	157.1	100.5	120	30	575	575
	A8	200	150	54.00	157.1	100.5	120	30	575	575
	A9	200	150	54.00	157.1	100.5	120	30	575	575
	A10	200	150	54.00	157.1	100.5	120	30	575	575
	A11	200	150	54.00	157.1	100.5	120	30	575	575
	B3	200	150	54.00	157.1	100.5	120	30	575	575
	B4	200	150	54.00	157.1	100.5	120	30	575	575
	B5	200	150	54.00	157.1	100.5	120	30	575	575
	B6	200	150	54.00	157.1	100.5	120	30	575	575
	B7	200	150	54.00	157.1	100.5	120	30	575	575
	B8	200	150	54.00	157.1	100.5	120	30	575	575
	C3	200	150	54.00	401.9	100.5	120	30	575	575
	C4	200	150	54.00	401.9	100.5	120	30	575	575
	C5	200	150	54.00	401.9	100.5	120	30	575	575
	C6	200	150	54.00	401.9	100.5	120	30	575	575
	C7	200	150	54.00	401.9	100.5	120	30	575	575
	C8	200	150	54.00	401.9	100.5	120	30	575	575
[38]	DF.2	125	225	46.00	151	57	193	32	568	553
	DF.3	125	225	46.00	151	57	193	32	568	553
	DF.4	125	225	46.00	151	57	193	32	568	553
	AF3	125	225	46.00	151	57	193	32	568	553
	CF2-1	125	225	46.00	151	57	193	32	568	553
	CF3-1	125	225	46.00	151	57	193	32	568	553
	CF4-1	125	225	46.00	151	57	193	32	568	553
	VR5	120	250	33.60	157	57	214	34	565	738
	VR6	120	250	33.60	157	57	214	34	565	738
	VR7	120	250	33.60	157	57	214	34	565	738
	VR8	120	250	33.60	157	57	214	34	565	738
	VR9	120	250	33.60	157	57	214	34	565	738
	VR10	120	250	33.60	157	57	214	34	565	738
	A3	150	300	51.70	792	–	250	–	427	–
	A8	150	300	51.70	792	–	250	–	427	–
	C2	150	300	51.70	792	–	250	–	427	–
	C	152	305	39.80	253	–	251	30.5	414	–
	D	152	305	39.80	253	–	251	30.5	414	–
	G	152	305	43.00	253	–	251	30.5	414	–
	I	152	305	39.80	253	–	251	30.5	414	–
	M	152	305	43.00	253	–	251	30.5	414	–
	B2	100	100	43.99	85	57	84	16	350	350
	B3	100	100	43.99	85	57	84	16	350	350
	B4	100	100	43.99	85	57	84	16	350	350
	B6	100	100	43.99	85	57	84	16	350	350
	1Au	100	100	49.05	85	57	84	16	350	350
	1Bu	100	100	49.05	85	57	84	16	350	350
	1B2u	100	100	49.05	85	57	84	16	350	350
	1Cu	100	100	49.05	85	57	84	16	350	350
	2Au	100	100	49.05	85	57	84	16	350	350
	2Bu	100	100	49.05	85	57	84	16	350	350
	2Cu	100	100	49.05	85	57	84	16	350	350
	3Au	100	100	49.05	85	57	84	16	350	350
	3Bu	100	100	49.05	85	57	84	16	350	350
	3Cu	100	100	49.05	85	57	84	16	350	350
	B1U, 2.3	130	230	39.01	236	101	206	25	556	556
	P2	150	300	40.00	308	–	257	30	500	–
	P3	150	300	40.00	308	–	257	30	500	–
	P4	150	300	40.00	308	–	257	30	500	–
	P5	150	300	40.00	308	–	257	30	500	–
	2	150	250	36.77	157	157	205	45	537	537
	4	150	250	37.60	157	157	205	45	537	537
	5	150	250	42.16	157	157	205	45	537	537

Table A.3 (*continued*)

References	Specimen name	Concrete			Steel reinforcement					
		b (mm)	h (mm)	f_c (MPa)	A_s (mm^2)	A'_s (mm^2)	d_s (mm)	d'_s (mm)	f_y (MPa)	f'_y (MPa)
	6	150	250	41.42	157	157	205	45	537	537
	7	150	250	39.01	157	157	205	45	537	537
	B	205	455	35	1013	253	400	55	456	456
	SB1	200	300	53.12	402	402	252	48	527	527
	SB2	200	300	53.95	402	402	252	48	527	527
	SB3	200	300	53.95	402	402	252	48	527	527
	MB1	200	300	58.10	402	402	252	48	527	527
	HB1	200	300	58.10	402	402	252	48	527	527
	FB1	200	300	53.12	402	402	252	48	527	527
	B7	75	150	37	14	151	131	22	190	470
	1B	200	200	54.8	143	143	152	48	410	410
	1C	200	200	54.8	143	143	152	48	410	410
	2B	200	200	54.8	253	143	152	48	410	410
	2C	200	200	54.8	253	143	152	48	410	410
	2D	200	200	54.8	253	143	152	48	410	410
	3B	200	200	54.8	396	143	152	48	410	410
	3C	200	200	54.8	396	143	152	48	410	410
	3D	200	200	54.8	396	143	152	48	410	410
[39]	A1	150	300	51.70	792	–	250	–	427	–
	A2	200	200	51.70	792	–	251	–	427	–
	A7	200	200	51.70	792	–	252	–	427	–
	C1	200	200	51.70	792	–	253	–	427	–
	B2	270	400	22.60	900	142	341	54	484	507
	CS1	303	150.8	22.24	157	–	115.3	–	343	–
	GS1	302	151.2	23.41	157	–	117.9	–	343	–
	E	205	455	35	253	–	400	–	456	–
	B1u, 4.5	145	230	39.01	33	–	114	–	517	–
	4	76	127	44.7	33	–	111	–	517	–
	5	76	127	44.7	33	–	112	–	517	–
	6	76	127	44.7	33	–	113	–	517	–
	7	76	127	44.7	33	–	114	–	517	–
	8	76	127	44.7	33	–	115	–	517	–
	CP1	301.5	150.5	28.05	314	–	117.4	–	343	–
	CP2	303.6	151.9	39.09	314	–	111.3	–	343	–
	CP3	302.7	150	13.11	157	–	108.2	–	343	–
	CP5	304	149	26.56	157	–	117.4	–	355	–
[40]	Cantilever 1U	100	100	64	157.1	226.2	90	10	350	350
	Cantilever 1A	100	100	64	157.1	226.2	90	10	350	350
	Cantilever 2U	100	100	64	157.1	226.2	90	10	350	350
	Cantilever 4U	100	100	64	157.1	226.2	90	10	350	350
	Cantilever 5U	100	100	64	157.1	226.2	90	10	350	350
	Cantilever 2A	100	100	64	157.1	226.2	90	10	350	350
[42][a]	A950	120	150	32.1	236	57	120	25	384	400
	A1100	120	150	32.1	236	57	120	25	384	400
	A1150	120	150	32.1	236	57	120	25	384	400
	B1	120	150	44.6	57	57	120	27	400	400
	B2[a]	120	150	44.6	628	57	120	20	466	400
	C5[a]	120	150	25.1	236	57	140	5	384	400
	C10[a]	120	150	25.1	236	57	135	10	384	400
	C20[a]	120	150	25.1	236	57	125	20	384	400

[a] Not used for the bond strength models assessment.

Table A.4
Geometrical and mechanical characteristics of the FRP strengthening used for the RC beams tested in bending (Table A.3).

References	Specimen name	FRP strengthening							Test results	
		FRP	n	t_f (mm)	b_f (mm)	l_b (mm)	E_f (MPa)	f_f (MPa)	P_u (kN)	l_e (mm)
[35]	AF.2	C_S	2	0.167	75	1100	2,40,000	3500	83.00	–
	AF.2-1	C_S	2	0.167	75	1200	2,40,000	3500	85.70	–
	AF.4	C_S	2	0.167	75	1400	2,40,000	3500	111.00	–
	DF.1	C_S	1	0.167	75	1400	2,40,000	3500	118.00	–
[36]	F5	C_L	1	1.2	120	2030	1,55,000	2400	100.00	–
	F6	C_L	1	1.2	120	2030	1,55,000	2400	103.00	–
	F7	C_L	1	1.2	120	1876	1,55,000	2400	97.50	–
	F8	C_L	1	1.2	120	1876	1,55,000	2400	64.00	–
	F9	C_L	1	1.2	120	1700	1,55,000	2400	62.00	–
	F10	C_L	1	1.2	120	1700	1,55,000	2400	82.00	–

(*continued on next page*)

Table A.4 (*continued*)

References	Specimen name	FRP strengthening							Test results	
		FRP	n	t_f (mm)	b_f (mm)	l_b (mm)	E_f (MPa)	f_f (MPa)	P_u (kN)	l_e (mm)
[37]	A4	C_S	4	0.2	150	1930	1,27,000	1532	61.90	–
	A5	C_S	4	0.2	150	1930	1,27,000	1532	63.20	–
	A6	C_S	6	0.2	150	1930	1,27,000	1532	59.40	–
	A7	C_S	6	0.2	150	1930	1,27,000	1532	70.60	–
	A8	C_S	4	0.2	150	1930	1,27,000	1532	65.20	–
	A9	C_S	4	0.2	150	1930	1,27,000	1532	63.90	–
	A10	C_S	4	0.2	150	1930	1,27,000	1532	67.50	–
	A11	C_S	4	0.2	150	1930	1,27,000	1532	69.40	–
	B3	C_S	2	0.2	150	1930	1,27,000	1532	55.20	–
	B4	C_S	2	0.2	150	1930	1,27,000	1532	52.50	–
	B5	C_S	6	0.2	150	1930	1,27,000	1532	69.70	–
	B6	C_S	6	0.2	150	1930	1,27,000	1532	69.60	–
	B7	C_S	12	0.15	150	1930	1,27,000	1532	59.10	–
	B8	C_S	12	0.15	150	1930	1,27,000	1532	61.60	–
	C3	C_S	2	0.2	150	1930	1,27,000	1532	74.90	–
	C4	C_S	2	0.2	150	1930	1,27,000	1532	77.52	–
	C5	C_S	6	0.2	150	1930	1,27,000	1532	103.10	–
	C6	C_S	6	0.2	150	1930	1,27,000	1532	101.40	–
	C7	C_S	12	0.15	150	1930	1,27,000	1532	87.10	–
	C8	C_S	12	0.15	150	1930	1,27,000	1532	86.70	–
[38]	DF.2	C_S	2	0.167	75	1400	240,000	3500	60.30	–
	DF.3	C_S	3	0.167	75	1400	240,000	3500	60.00	–
	DF.4	C_S	4	0.167	75	1400	240,000	3500	62.80	–
	AF3	C_S	2	0.167	75	1300	240,000	3500	48.30	–
	CF2-1	C_S	2	0.167	75	1300	240,000	3500	52.40	–
	CF3-1	C_S	2	0.167	75	1300	240,000	3500	59.10	–
	CF4-1	C_S	2	0.167	75	1300	240,000	3500	70.10	–
	VR5	C_S	4	0.11	120	2200	230,000	3400	51.10	–
	VR6	C_S	4	0.11	120	2200	230,000	3400	50.30	–
	VR7	C_S	7	0.11	120	2200	230,000	3400	62.10	–
	VR8	C_S	7	0.11	120	2200	230,000	3400	62.00	–
	VR9	C_S	10	0.11	120	2200	230,000	3400	64.80	–
	VR10	C_S	10	0.11	120	2200	230,000	3400	68.50	–
	A3	C_S	3	0.165	150	2130	230,000	3400	86.10	–
	A8	C_S	6	0.165	75	2130	230,000	3400	98.20	–
	C2	C_S	3	0.165	150	2130	230,000	3400	79.30	–
	C	G_L	1	4.76	152	2032	11,720	161	55.40	–
	D	G_L	1	4.76	151	2032	11,720	161	59.60	–
	G	G_L	1	4.19	152	2438	10,340	184	62.90	–
	I	C_L	1	4.06	150	2032	27,580	319	50.60	–
	M	C_L	1	1.27	152	2438	1,17,900	1489	72.10	–
	B2	G_L	1	1.2	80	860	49,000	1078	17.00	–
	B3	G_L	1	1.2	30	860	49,000	1078	12.30	–
	B4	G_L	1	1.6	60	860	49,000	1078	17.50	–
	B6	C_L	1	1.2	80	860	1,18,500	987	20.40	–
	1Au	C_L	1	0.5	90	860	1,11,000	1273	19.80	–
	1Bu	C_L	1	0.7	65	860	1,11,000	1273	18.30	–
	1B2u	C_L	1	0.7	65	860	1,11,000	1273	18.20	–
	1Cu	C_L	1	1	45	860	1,11,000	1273	16.00	–
	2Au	C_L	1	0.5	90	860	1,11,000	1273	19.30	–
	2Bu	C_L	1	0.7	65	860	1,11,000	1273	17.00	–
	2Cu	C_L	1	1	45	860	1,11,000	1273	17.80	–
	3Au	C_L	1	0.5	90	861	1,11,000	1273	19.50	–
	3Bu	C_L	1	0.7	65	862	1,11,000	1273	17.30	–
	3Cu	C_L	1	1	45	863	1,11,000	1273	15.40	–
	B1U, 2.3	C_L	1	1.28	90	2120	1,15,000	1284	50.20	–
	P2	C_L	1	1.2	100	2400	1,50,000	2400	68.00	–
	P3	C_L	1	1.2	100	2400	1,50,000	2400	71.10	–
	P4	C_L	1	2.4	100	2400	1,50,000	2400	78.00	–
	P5	C_L	1	2.4	100	2400	1,50,000	2400	79.50	–
	2	G_L	1	1.32	150	800	19,720	259	53.00	–
	4	G_L	1	1.32	150	1100	19,720	259	65.40	–
	5	G_L	1	2.64	150	1400	19,720	259	79.40	–
	6	G_L	1	1.32	150	1100	19,720	259	63.10	–
	7	G_L	1	1.32	150	800	19,720	259	53.90	–
	B	G_L	1	6	152	4265	3,72,300	400	125.00	–
	SB1	C_L	1	1.4	120	3300	1,55,000	2400	71.40	–
	SB2	C_L	1	1.4	120	3200	1,55,000	2400	75.50	–
	SB3	C_L	1	1.4	120	3000	1,55,000	2400	73.90	–
	MB1	C_L	1	1.4	120	3300	2,10,000	2000	79.60	–
	HB1	C_L	1	1.4	100	3300	3,00,000	1400	80.10	–
	FB1	C_L	1	2.4	150	3300	95,000	1800	74.40	–
	B7	C_L	1	1.2	50	1480	1,50,000	2400	12.50	–
	1B	C_L	1	0.45	200	2740	1,38,000	2206	40.10	–

Table A.4 (*continued*)

References	Specimen name	FRP strengthening							Test results	
		FRP	n	t_f (mm)	b_f (mm)	l_b (mm)	E_f (MPa)	f_f (MPa)	P_u (kN)	l_e (mm)
	1C	C_L	1	0.45	200	2740	1,38,000	2206	35.60	–
	2B	C_L	1	0.45	200	2740	1,38,000	2206	49.00	–
	2C	C_L	1	0.45	200	2740	1,38,000	2206	35.60	–
	2D	C_L	1	0.45	200	2740	1,38,000	2206	40.10	–
	3B	C_L	1	0.45	200	2740	1,38,000	2206	54.50	–
	3C	C_L	1	0.45	200	2740	1,38,000	2206	54.10	–
	3D	C_L	1	0.45	200	2740	1,38,000	2206	54.30	–
[39]	A1	C_S	3	0.165	150	2130	2,30,000	3400	86.10	–
	A2	C_S	6	0.165	75	2130	2,30,000	3400	98.20	–
	A7	C_S	3	0.165	150	2130	2,30,000	3400	79.30	–
	C1	C_S	1	0.165	150	2130	2,30,000	3400	72.80	–
	B2	C_S	2	0.165	150	2130	2,30,000	3400	84.90	–
	CS1	C_S	2	0.165	75	2130	2,30,000	3400	86.10	–
	GS1	G_S	1	0.165	150	2130	2,30,000	3400	77.20	–
	E	G_L	1	6	152	4265	37,200	400	32.50	–
	B1u, 4.5	C_L	1	1.28	90	4320	1,15,000	1284	30.00	–
	4	C_L	1	0.65	63.2	1070	1,86,000	1450	14.80	–
	5	C_L	1	0.65	63.2	1070	1,86,000	1450	15.30	–
	6	C_L	1	0.9	63.3	1070	1,86,000	1450	14.00	–
	7	C_L	1	0.9	63.3	1070	1,86,000	1450	12.80	–
	8	C_L	1	1.9	63.9	1070	1,86,000	1450	18.70	–
	CP1	C_L	1	1.2	50	900	1,65,000	2800	19.95	–
	CP2	C_L	1	12.2	50	900	1,65,000	2800	17.58	–
	CP3	C_L	1	1.2	50	900	1,65,000	2800	13.31	–
	CP5	C_L	1	1.2	50	900	1,65,000	2800	10.00	–
[40]	Cantilever 1U	C_L	1	0.82	67	920	1,11,000	1414	16.45	–
	Cantilever 1A	C_L	1	0.82	67	920	1,11,000	1414	32.45	–
	Cantilever 2U	C_L	1	0.82	67	920	1,11,000	1414	19.31	–
	Cantilever 4U	C_L	1	0.82	67	920	1,11,000	1414	15.43	–
	Cantilever 5U	C_L	1	0.82	67	920	1,11,000	1414	11.33	–
	Cantilever 2A	C_L	1	0.82	67	920	1,11,000	1414	11.59	–
[42][a]	A950	C_L	1	1.2	80	950	1,8,000	3140	56.2	250
	A1100	C_L	1	1.2	80	1100	1,81,000	3140	57.3	250
	A1150	C_L	1	1.2	80	1150	1,81,000	3140	58.9	250
	B1	C_L	1	1.2	80	1100	1,81,000	3140	49.2	250
	B2[a]	C_L	1	1.2	80	1100	1,81,000	3140	130.1	220
	C5[a]	C_L	1	1.2	80	1100	1,81,000	3140	71	240
	C10[a]	C_L	1	1.2	80	1100	1,81,000	3140	68	240
	C20[a]	C_L	1	1.2	80	1100	1,81,000	3140	63	240

[a] Not used for the bond strength models assessment.

References

[1] Consiglio Nazionale delle Ricerche (CNR). Instructions for design, execution and control of strengthening interventions through fiber-reinforced composites. CNR-DT 200-04. Consiglio Nazionale delle Ricerche, Rome, Italy; 2004.

[2] Pellegrino C, Modena C. FRP shear strengthening of RC beams with transverse steel reinforcement. J Compos Constr 2002;6(2):104–11.

[3] Pellegrino C, Modena C. FRP shear strengthening of RC beams: experimental study and analytical modelling. ACI Struct J 2006;103(5):720–8.

[4] Pellegrino C, Modena C. An experimentally based analytical model for shear capacity of FRP strengthened reinforced concrete beams. Mech Compos Mat 2008;44(3):231–44.

[5] Pellegrino C, Modena C. Flexural strengthening of real-scale RC and PRC beams with end-anchored pre-tensioned FRP laminates. ACI Struct J 2009;106(3):319–28.

[6] Valluzzi MR, Grinzato E, Pellegrino C, Modena C. IR thermography for interface analysis of FRP laminates externally bonded to RC beams. Mat Struct 2009;42(1):25–34.

[7] Lam L, Teng JG. Design-oriented stress–strain model for FRP-confined concrete. Constr Build Mat 2003;17(6–7):471–89.

[8] Pellegrino C, Modena C. Analytical model for FRP confinement of concrete columns with and without internal steel reinforcement. J Compos Constr ASCE 2010;14(6):693–705.

[9] Taljsten B. Defining anchor lengths of steel and CFRP plates bonded to concrete. Int J Adhes Adhes 1997;17(4):319–27.

[10] Bizindavyi L, Neale KW. Transfer lengths and bond strengths for composites bonded to concrete. J Compos Constr ASCE 1999;3(4):153–60.

[11] Chen JF, Teng JG. Anchorage strength models for FRP and steel plates bonded to concrete. J Struct Eng ASCE 2001;127(7):784–91.

[12] Nakaba K, Kanakubo T, Furuta T, Yoshizawa H. Bond behaviour between fiber-reinforced polymer laminates and concrete. ACI Struct J 2001;98(3):359–67.

[13] Lu XZ, Teng JG, Ye LP, Jiang JJ. Bond–slip models for FRP sheets/plates bonded to concrete. Eng Struct 2005;27:920–37.

[14] Pellegrino C, Tinazzi D, Modena C. Experimental study on bond behavior between concrete and FRP Reinforcement. J Compos Constr ASCE 2008;12(2):180–9.

[15] Yuan H, Teng JG, Seracino R, Wu ZS, Yao J. Full-range behavior of FRP-to-concrete bonded joints. Eng Struct 2004;26(5):553–64.

[16] fib Bulletin 14. Externally bonded FRP reinforcement for RC structures. Lausanne, Switzerland; 2001.

[17] American Concrete Institute (ACI). Guide for the design and construction of externally bonded FRP systems for strengthening of concrete structure. ACI 440.2R-08, Farmington Hill, Michigan; 2008.

[18] Consiglio Nazionale delle Ricerche (CNR). Istruzioni per la progettazione, l'esecuzione ed il controllo di interventi di consolidamento statico mediante l'utilizzo di compositi fibrorinforzati. CNR-DT 200 R1/2013. Consiglio Nazionale delle Ricerche, Rome, Italy; 2013.

[19] Van Gemert D. Force transfer in epoxy-bonded steel–concrete joints. Int J Adhes Adhes 1980;1:67–72.

[20] Hiroyuki Y, Wu Z. Analysis of debonding fracture properties of CFS strengthened member subject to tension. In: Proceedings of 3rd international symposium on non-metallic (FRP) reinforcement for concrete structures, vol. 1; 1997. p. 284–94.

[21] Neubauer U, Rostàsy FS. Design aspects of concrete structures strengthened with externally bonded CFRP plates. In: Proceedings of seventh international conference on structural faults and repairs. Edinburgh, ECS Publications, vol. 1; 1997. p. 109–18.

[22] Khalifa A, Gold WJ, Nanni A, Aziz A. Contribution of externally bonded FRP to shear capacity of RC flexural members. J Compos Constr ASCE 1998;2(4):195–203.

[23] Adhikary BB, Mutsuyoshi H. Study on the bond between concrete and externally bonded CFRP sheet. In: Proceedings of the 6th international symposium on fiber reinforced polymer reinforcement for concrete structures, FRPRCS-5, vol. 1, 2001. p. 371–78.
[24] De Lorenzis L, Miller B, Nanni A. Bond of fiber-reinforced polymer laminates to concrete. ACI Mater J 2001;98(3):256–64.
[25] Japan Concrete Institute (JCI). Technical report of technical committee on retrofit technology. In: Proceedings of the international symposium on latest achievement of technology and research on retrofitting concrete structures; 2003.
[26] Dai J, Ueda T, Sato Y. Development of the nonlinear bond stress–slip model of fiber reinforced plastics sheet-concrete interfaces with a simple method. J Compos Constr ASCE 2005;9(1):52–62.
[27] Camli US, Binici B. Strength of carbon fiber reinforced polymers bonded to concrete and masonry. Constr Build Mat 2007;21:1431–46.
[28] Yao J, Teng JG, Chen JF. Experimental study on FRP-to-concrete bonded joints. Compos B: Eng 2005;36:99–113.
[29] Toutanji H, Saxena P, Zhao L, Ooi T. Prediction of interfacial bond failure of FRP—Concrete surface. J Compos Constr ASCE 2007;11(4):427–36.
[30] Ceroni F, Pecce M. Evaluation of bond strength in concrete element externally reinforced with CFRP sheets and anchoring devices. J Compos Constr ASCE 2010;14(5):521–30.
[31] Subramaniam KV, Carloni C, Nobile L. Width effect in the interface fracture during shear debonding of FRP sheets from concrete. Eng Fract Mech 2007;74:578–94.
[32] Subramaniam KV, Carloni C, Nobile L. An understanding of the width effect in FRP–concrete debonding. Strain 2011;47:127–37.
[33] Carloni C, Subramaniam KV, Savoia M, Mazzotti C. Experimental determination of FRP–concrete cohesive interface properties under fatigue loading. Compos Struct 2012;94:1288–96.
[34] Carloni C, Subramaniam K. Investigation of sub-critical fatigue crack growth in FRP/concrete cohesive interface using digital image analysis. Compos B: Eng 2013;51:35–43.
[35] Ahmed O, van Gemert D, Vanderwalle L. Improved model for plate end shear of CFRP strengthened RC beams. Cem Concr Compos 2001;23(1):3–19.
[36] Fanning PJ, Kelly O. Ultimate response of RC beams strengthened with CFRP plates. J Compos Constr ASCE 2001;5(2):122–7.
[37] Rahimi H, Hutchinson A. Concrete beams strengthened with externally bonded FRP plates. J Compos Constr ASCE 2001;5(1):44–56.
[38] Smith ST, Teng JG. FRP-strengthened RC beams-II: assessment of debonding strength models. Eng Struct 2002;24(4):397–417.
[39] Teng JG, Smith ST, Yao J, Chen JF. Intermediate crack-induced in RC beams and slabs. Constr Build Mater 2003;17:447–62.
[40] Garden HN, Hollaway LC. An experimental study of the influence of plate end anchorage of carbon fibre composite plates used to strengthen reinforced concrete beams. Compos Struct 1998;42:175–88.
[41] Pellegrino C, Vasic M. Assessment of design procedures for the use of externally bonded FRP composites in shear strengthening of reinforced concrete beams. Compos B: Eng 2013;45(1):727–41.
[42] Nguyen DM, Chan TK, Cheong HK. Brittle failure and bond development length of CFRP–concrete beams. J Compos Constr ASCE 2001;5(1):12–7.